Multi-transformer primary-side regulated flyback converter for supplying isolated IGBT and MOSFET drivers

Maciej Kolincio, *Student Member, IEEE*, Piotr J. Chrzan, *Senior Member, IEEE* and Piotr Musznicki

Abstract—This paper presents primary-side voltage regulated multi-transformer quasi-resonant flyback converter (MTFC) for supplying isolated power switch drivers. The proposed topology offers distinct advantages over frequently used flyback converter possessing one high frequency transformer with isolated multiple outputs. Particularly, when a large number of separate dc supply units is required, then MTFC enables improved regular distribution of magnetic coupling between the common primary and the multiple secondary transformers' windings providing high degree of galvanic and electromagnetic isolation between multiple outputs. Primary side voltage regulation is based on the average output voltage estimation using auxiliary RDC circuit mounted across the primary windings. Operation principles of MTFC are enhanced with analytical study of cross regulation of multiple output voltages at unbalanced load conditions, indicating reduced voltage deviation of multiple outputs by applying the primary-side average voltage regulation. Experimental results of prototype 2, 3, and 6-transformer quasi-resonant flyback converters confirmed their cross regulation quality and application potential for independent multiple output supplies.

Index Terms—quasi-resonant flyback control, multiple output dc supply, power switch drivers, cross regulation.

I. INTRODUCTION

Multiple output switch mode power supplies are widely applied in power electronics converters, aerospace and computer systems, since they are more compact with less number of components than independent single-output supplies. Particular application domain has evolved for supplying isolated IGBT and MOSFET power switch drivers. Recently developed topologies of multilevel converters, matrix converters or battery management systems need a large number of power switches with galvanic isolated supply of switch drivers. For reliable switching operation, they usually require both positive and negative voltages in the range of $\pm$ 10-15 V [1]. Some cost effective methods to power the gate drivers use the bootstrap techniques [2], [3], however they require prescribed converter switching sequence and producing negative bias rail needs auxiliary circuit build up. The most accepted solution offers

the multi-output flyback converter (MOFC) consisted of one high frequency transformer with isolated multiple secondary outputs, depicted in Fig. 1a [4], [5]. Regulation of the MOFC
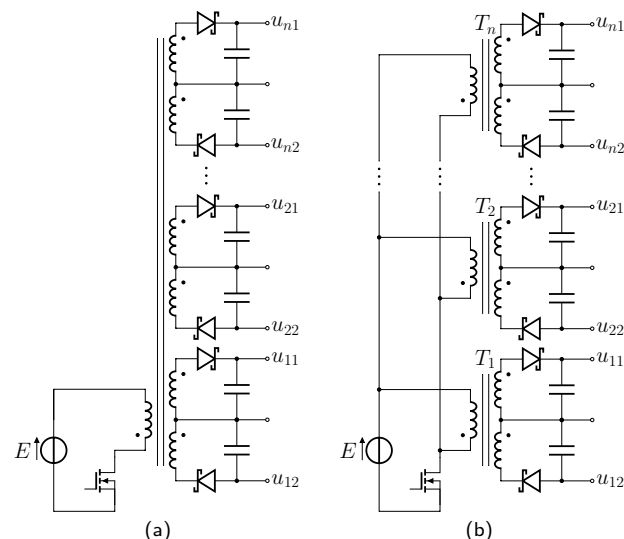

Fig. 1. Flyback converter with multiple bipolar outputs; a) transformer with multi-winding secondary, b) multi-transformer topology.

is based on the selected output voltage control loop and cross regulation of other independent multi-output supply channels [6]. Measurement of output voltage is usually realized by an opto-coupler feedback circuit or by the auxiliary transformer winding [7]–[9]. Output voltage value can also be obtained by sampling primary winding voltage [10]. In order to improve efficiency and minimize electromagnetic interference (EMI), the quasi-resonant (QR) control of the MOFC has been applied [11]. When the secondary-side diodes turn off, the transistor switch drain node starts to oscillate. The switch turns on when its drain voltage reaches the minimum level. This is called the valley switching mode. Converter operates at the boundary conduction mode (BCM) by employing variable frequency operation, depending on load conditions. Recent control issues limit increase of that frequency at light load by skipping some valleys [12], [13]. If a large numbers of isolated multiple outputs of MOFC are required, it becomes difficult with secondary windings placement to assure proper isolation, equal magnetic coupling and minimal leakage fluxes for each winding. Otherwise, it decreases a quality of cross-regulation of multiple outputs. Moreover, the transformer

volume will increase. So far, multiple transformer converters with parallel-series transformer have been used for decreasing dimensions [14] or increasing voltage ratio [15]. Recently, multi-transformer based LLC resonant half-bridge converter has been applied for isolated gate drivers power supply. To minimize capacitive coupling between secondary and primary side, this converter operates in the open loop resonant mode, requiring however a precise dimensioning and quality of components of the resonant tank [16]

In this paper a new multiple transformer flyback converter (MTFC) topology is proposed, as in Fig. 1b [17]. Each transformer unit Ti generates a pair of symmetric positive and negative voltages with floating g round f or independent switch drivers supply. All transformers primary windings are connected in parallel circuit with the series connection of the dc input voltage E and the MOSFET switch. The papers objective is to demonstrate efficiency o f t he M TFC primary side regulation, that is based on the average output voltage estimation, obtained by the auxiliary RDC circuit mounted across the primary transformer windings. In the following paper sections, the MTFC is analytically and experimentally investigated with a reference to the cross regulation quality at variable load conditions of individual outputs.

II. ANALYSIS OF MTFC

We start circuit-oriented analysis of n-transformer MTFC model as in Fig.1b) with unipolar output voltage circuits and the following assumptions:

- MTFC transistor switch is represented by ideal switch Q;
- secondary diode forward voltage and equivalent series resistance are neglected
- all transformers T_1-T_n have identical turns ratio ϑ=n1/n2 and other parameters;
- equivalent transformer leakage inductances L_l are referred to the primary winding, transformer magnetizing inductances L_m are constant, winding resistances are neglected;
- due to large output capacitances, the output voltages are constant within the MTFC operation cycle and can be replaced by equivalent voltage sources u_{o1} ... u_{on};

Furthermore, assuming equal load resistances R_{oi} (i=2,..N) of n-1 transformers we replace them by one equivalent transformer T_z, where

$$L_{mz} = \frac{L_m}{n-1} \qquad (1)$$

$$L_{lz} = \frac{L_l}{n-1} \qquad (2)$$

and

$$R_{oz} = \frac{R_{o2}}{n-1} \qquad (3)$$

Thus, n-transformer MTFC model can be considered by equivalent 2-transformers MTFC consisting of T_1 and T_z units, as is depicted in Fig. 2. In this model, load resistance R_{o1} of the first transformer T_1 unit may vary with rapport to the constant load resistance R_{oz} of equivalent unit T_z.

Without loss of generality we assume, that $R_{o1} < R_{oz}$(n-1) is leading to unequal output voltages distribution (u_{o1}<u_{oz}).
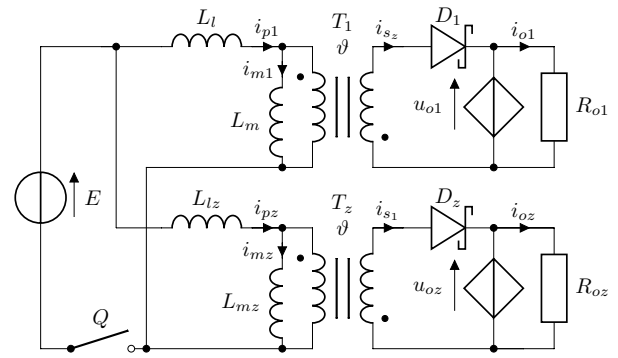

Fig. 2. MTFC – two transformers equivalent model.

TABLE I
MTFC SWITCHING STATES AT UNBALANCED LOAD CONDITIONS.

	Q	D_1	D_z
I	1	0	0
II	0	1	1
III	0	1	0

Then, in one operation cycle, based on states of the switch Q and of the secondary diodes D_1, D_z, three modes can be distinguished (Table I). Corresponding to these modes: primary i_{p1}, i_{pz} and secondary i_{s1}, i_{sz} transformer current transients are illustrated in Fig. 3.

A. Timing Relationships

Mode I (t_0<t<t_1)

Switch Q is turned on. Voltage across primary transformer windings is equal the source voltage E. Primary currents linearly augment

$$\frac{di_{p1}}{dt} = \frac{E}{L_m + L_l} \qquad (4)$$

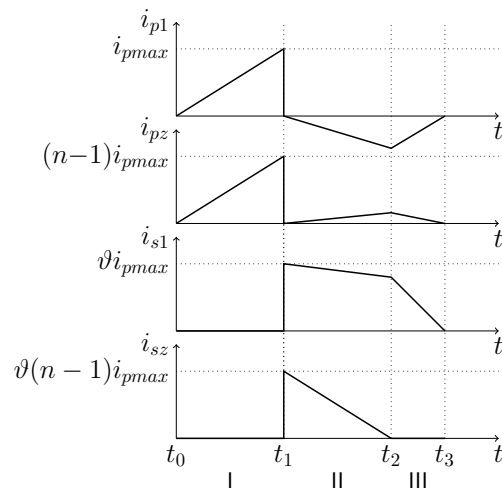$$\frac{di_{pz}}{dt} = \frac{E}{L_{mz} + L_{lz}} \qquad (5)$$

Fig. 3. Transformer current transients for one operation cycle at unbalanced load conditions.

The switch Q is turned off for $t = t_1$ when its current reaches the maximal value ni_{pmax}. Hence, the time interval of mode I

$$T_I = i_{pmax}\frac{L_m + L_l}{E} \quad (6)$$

Mode II ($t_1 < t < t_2$)

Secondary diodes start to conduct. Energy accumulated in transformers is transferred to secondary load circuits. Due to unbalanced load conditions, the compensation current component flows between the primary transformer circuits. Conserving signs of current components as in Fig. 2, yields

$$(L_l + L_{lz})\frac{di_{p1}}{dt} + \vartheta(u_{oz} - u_{o1}) = 0 \quad (7)$$

$$L_m\frac{di_{m1}}{dt} + \vartheta u_{o1} = 0 \quad (8)$$

$$L_{mz}\frac{di_{mz}}{dt} + \vartheta u_{oz} = 0 \quad (9)$$

Since secondary currents consist of two components

$$i_{s1} = \vartheta(i_{m1} - i_{p1}) \quad (10)$$

$$i_{sz} = \vartheta(i_{mz} + i_{p1}) \quad (11)$$

the following secondary current equations are deriveds

$$\frac{di_{s1}}{dt} = -\frac{\vartheta^2 u_{o1}}{L_m} + \frac{\vartheta^2(u_{oz} - u_{o1})}{L_l + L_{lz}} \quad (12)$$

$$\frac{di_{sz}}{dt} = -\frac{\vartheta^2 u_{oz}}{L_{mz}} - \frac{\vartheta^2(u_{oz} - u_{o1})}{L_l + L_{lz}} \quad (13)$$

The second subcycle ends when i_{sz} decreases to zero, hence the time interval of mode II

$$T_{II} = i_{pmax}\frac{nL_mL_l}{\vartheta(nu_{o1}L_l + \Delta u_o(L_m + nL_l))} \quad (14)$$

where

$$\Delta u_o = u_{oz} - u_{o1} \quad (15)$$

Mode III ($t_2 < t < t_3$)

Remaining energy of both transformers is transferred to more loaded secondary circuit of the T_1. Then, transient currents of primary and secondary circuits may be determined by the following equations

$$\frac{di_{p1}}{dt} = -\frac{di_{pz}}{dt} = \frac{\vartheta u_{o1}}{(L_{mz} + L_l + L_{lz})} \quad (16)$$

$$\frac{di_{s1}}{dt} = -\frac{\vartheta^2 u_{o1}}{L_m} - \frac{\vartheta^2 u_{o1}}{(L_{mz} + L_l + L_{lz})} \quad (17)$$

The third time interval T_{III} ends when i_{s1} decreases to zero, thus

$$T_{III} = \frac{i_{pmax}L_m\Delta u_o(nL_l + L_m)}{\vartheta nu_{o1}(u_{o1}L_l + \Delta u_o(L_m + nL_l))} \quad (18)$$

Hence, the total switching period of MTFC is given by

$$T_s = T_I + T_{II} + T_{III} \quad (19)$$

$$T_s = i_{pmax}\frac{EL_m + \vartheta u_{o1}(L_l + L_m)}{\vartheta E u_{o1}} \quad (20)$$

confirming its dependence on the primary maximal current i_{pmax}.

B. Energy Balance Relationships

Energy dissipated in loads of two transformer equivalent model are the following

$$W_{o1} = \frac{u_{o1}^2}{R_{o1}}T_s \quad (21)$$

$$W_{oz} = \frac{u_{oz}^2}{R_{oz}}T_s = (n-1)\frac{u_{oz}^2}{R_{o2}}T_s \quad (22)$$

Total energy stored in magnetizing inductances of MTFC in mode I is

$$W_I = \frac{(i_{p1}(t_1))^2}{2}L_m + \frac{(i_{pz}(t_1))^2}{2}L_{mz} \quad (23)$$

Next in mode II, transfer of energy to load of the transformer T_1 is calculated by

$$W_{II1} = u_{o1}i_{pmax}^2\frac{nL_mL_l(nu_{o1}L_l + \Delta u_o(2nL_l + (n+1)L_m)}{2(nu_{o1}L_l + \Delta u_o(L_m + nL_l))^2} \quad (24)$$

and respectively to the load of transformer T_z

$$W_{IIz} = (n-1)\frac{i_{pmax}^2 L_m}{2}\left(1 - \frac{\Delta u_o L_m}{(nu_{o1}L_l + \Delta u_o(L_m + nL_l))}\right) \quad (25)$$

Finally in mode III, the residual energy is transferred to the load of transformer T_1

$$W_{III1} = i_{pmax}^2\frac{n\Delta u_o^2 L_m(nL_l + L_m)(L_m + L_l)}{2(nu_{o1}L_l + \Delta u_o(L_m + nL_l))^2} \quad (26)$$

Hence, total energy that has been transferred to the T_1 load

$$W_1 = W_{II1} + W_{III_1} \quad (27)$$

and to the T_z load

$$W_z = W_{II_z} \quad (28)$$

From energy balance relationship

$$\begin{cases} W_{o1} = W_1 \\ W_{oz} = W_z \end{cases} \quad (29)$$

the following energy balance equation can be derived

$$\Delta u_o^2 R_{o1}(L_l + L_m) + \Delta u_o u_{o1}R_{o1}(2L_l + L_m) + u_{o1}^2(R_{o1} - R_{o2})L_l = 0 \quad (30)$$

Defining the relative leakage coefficient

$$K_1 = \frac{L_l}{L_m} \quad (31)$$

the load unbalance factor

$$K_2 = \frac{R_{o1}}{R_{o2}} \quad (32)$$

and calculating output voltage deviation Δu_o yields

$$\frac{\Delta u_o}{u_{o1}} = \frac{-(2K_1 + 1) + \sqrt{4\frac{K_1^2}{K_2} + 4\frac{K_1}{K_2} + 1}}{2(K_1 + 1)} \quad (33)$$

The case of reverse unbalance for $R_{o1} > R_{oz}(n-1)$, changes the direction of primary transformer currents transients, when the transistor Q is turned off. Then in mode III, remaining energy of both transformers is transferred to the

secondary circuit of the T_z feeding larger load. After repeating the analysis, complementary energy balance equation is obtained

$$\Delta u_o^2 R_{o2}(L_l + L_m) - \Delta u_o u_{oz} R_{o2}(2L_l + L_m) + \\ + u_{oz}^2 L_l(R_{o2} - R_{o1}) = 0 \qquad (34)$$

with resulting negative deviation voltage formula

$$\frac{\Delta u_o}{u_{oz}} = \frac{2K_1 + 1 - \sqrt{4K_1^2 K_2 + 4K_1 K_2 + 1}}{2(K_1 + 1)} \qquad (35)$$

Thus, one notes symmetry of voltage deviations for the load unbalance factor K_2 reverse change.

C. Output voltage deviation

If MTFC output voltages cross-regulation is based on the measurement of average voltage u_{oAV} of parallel connected primary transformer windings, then

$$u_{oAV} = \frac{u_{o1} + (n-1)u_{oz}}{n} = const \qquad (36)$$

Hence reformulating equation (33), output voltage deviation Δu_o is referred to the average voltage u_{oAV}

$$\Delta u_o = u_{oAV} \frac{n\left(-(2K_1+1)+\sqrt{4\frac{K_1^2}{K_2}+4\frac{K_1}{K_2}+1}\right)}{n+2K_1+1+(n-1)\sqrt{4\frac{K_1^2}{K_2}+4\frac{K_1}{K_2}+1}} \qquad (37)$$

and respectively for $R_{o1} > R_{oz}(n-1)$, from (35) as expressed by negative output voltage deviation

$$\Delta u_o = u_{oAV} \frac{n(2K_1+1-\sqrt{4K_1^2 K_2+4K_1 K_2+1})}{2n(K_1+1)-2K_1-1+\sqrt{4K_1^2 K_2+4K_1 K_2+1}} \qquad (38)$$

Two particular cases of load unbalance impact on voltage deviation are commonly represented for n=6 in Fig. 4. In the ideal case of zero transformer leakage inductance (K_1=0) or balanced load conditions (K_2=1), cross-regulation acts perfectly (Δu_o=0) . For typical transformer leakage coefficient in the range: 0.5-2%, Δu_o monotonically augments with K_2, however not exceeding ±15% for relatively wide load unbalance variations (K_2=0.1,...,10). Voltage deviation Δu_o sensitivity on a number of transformers n was calculated for extreme values in Fig. 4, corresponding to K_1=2% with unbalance factor K_2 changes from 0,1 to 10. It is evident, as depicted in Fig. 5, very low impact of number of transformers on voltage deviation Δu_o in the MTFC operation.

III. VOLTAGE CONTROL CIRCUIT IMPLEMENTATION

In the MTFC primary transformer windings are used for measurement of the average output voltage u_{oAV}. Measurement circuit consists of the R_1DC branch connected across the transformer winding (Fig.6). In order to verify the average output voltage estimation u_{oAV}, a complete MTFC model with the aid of the LTSpice XVII [18] circuit simulator was implemented, following the scheme presented in Fig. 6 and using parameter specification of the prototype circuit in Table II. Model consists of 6-transformer units with bipolar voltage outputs, the MOSFET based flyback converter, u_{oAV}
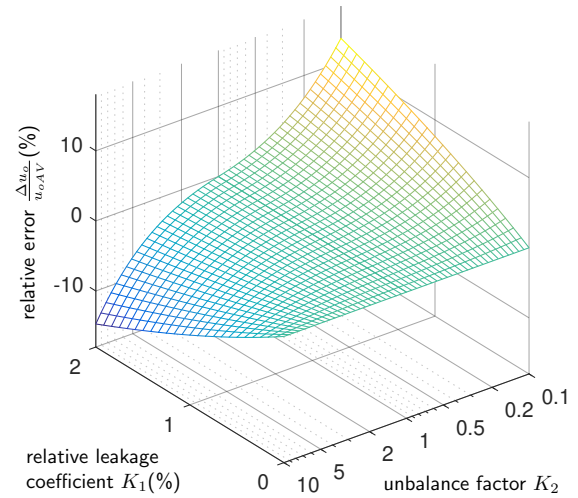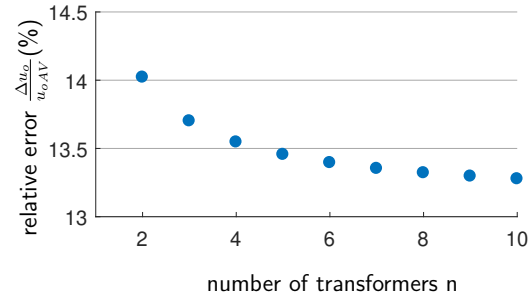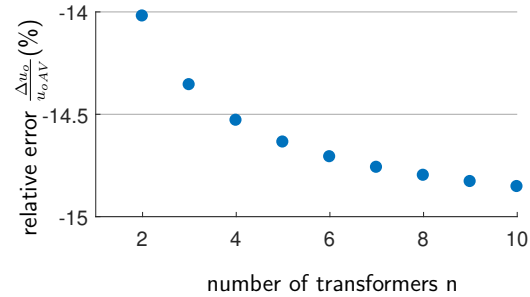

Fig. 4. MTFC relative voltage deviation (n=6)

(a)

(b)

Fig. 5. MTFC relative voltage deviation versus number of transformers; a) K_1=0.02, K_2=0.1; b) K_1=0.02, K_2=10

estimation block and the L6565 quasi resonant controller emulation circuit. Results of simulation of the primary voltage u_p and the capacitor voltage u_c are depicted in Fig. 7 in the same operation modes, as have been described in section II.

During mode I the u_p=-E, then the capacitor C discharges by the series connected resistors R_3 and R_5. In mode II at the MOSFET turn off, the R_1DC clamps the peak voltage on the drain and then the capacitor charges to the primary voltage $u_p = \vartheta u_{oAV}$ by the R_1D circuit. If mode III occurs, then $u_p < \vartheta u_{oAV}$, the capacitor C is discharged by the series
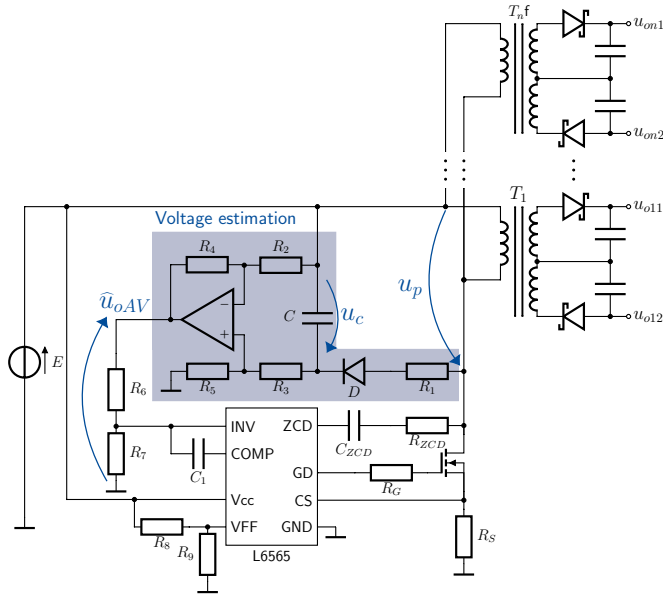
connected resistors: R_3 and R_5.

Fig. 6. Measurement scheme of average output voltage u_{oAV}.

$$C\frac{du_c}{dt} = \begin{cases} -\frac{E+u_c}{R_3+R_5} & \text{in mode I} \\ \frac{u_p-u_c}{R_1} - \frac{E+u_c}{R_3+R_5} & \text{in modes II-III} \end{cases} \quad (39)$$

The capacitor voltage u_c is next scaled in a differential amplifier, and the dc power supply voltage E is subtracted. Assuming equality of resistors ($R_2=R_3$; $R_4=R_5$) and appropriate selection of charging R_1C and discharging $(R_3+R_5)C$ time constants, the capacitor voltage u_c variations can be effectively filtered, providing the estimated output voltage $\widehat{u}_{oAV}$ free of swiching operation transients

$$\widehat{u}_{oAV} = u_c\frac{R_4}{R_2} \quad (40)$$

The voltage regulation is based on the L6565 quasi-resonant controller [7]. The voltage $\widehat{u}_{oAV}$ is fed to the L6565 voltage integral regulator through the resistor divider (R_6-R_7). The turn-off instant of the MOSFET switch is activated when its
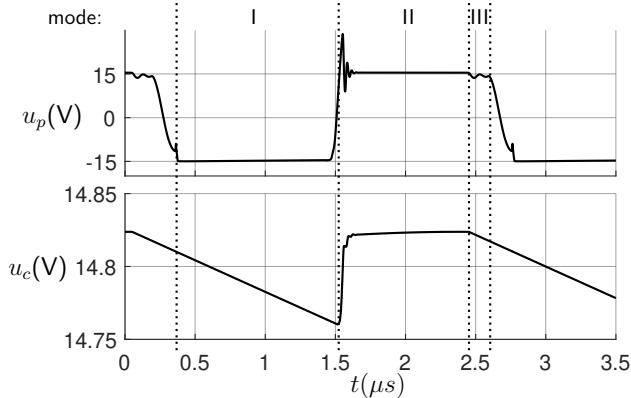

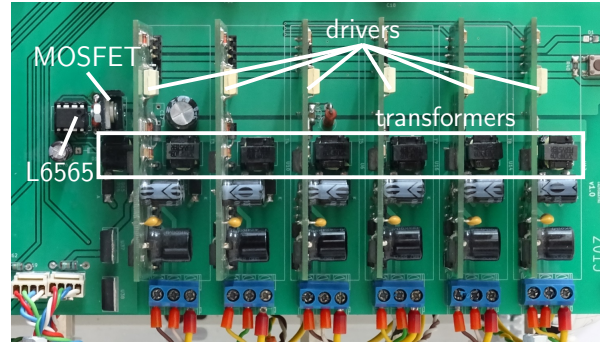Fig. 7. Simulating transients: u_p - primary voltage , u_c - capacitor voltage .

Fig. 8. MTFC prototype for 6 IGBT drivers supply with auxiliary unit for supplying LEM current sensors

TABLE II
PARAMETER SPECIFICATION OF THE MTFC PROTOTYPE CIRCUIT

Parameter	Symbol	Value
DC power supply	E	15 V
Switching frequency	f_s	180-700 kHz
MOSFET	–	IPB090N06N3
Diodes	–	SK110
Transformer	-	WE 750313972
Primary inductance	L_p	40 µH
Primary resistance	R_p	0.08 Ω
Secondary inductance	L_s	40 µH
Secondary resistance	R_s	0.185 Ω
Transformer ratio	ϑ	1
Leakage inductance @100 kHz	L_l	525 nH

current reaches the reference value ni_{pmax}, that is obtained from the voltage regulator. Estimate of instantaneous current is accomplished by measurement of the voltage at the current sense resistor R_S. Subsequent MOSFET turn-on instant is synchronized with the transformer demagnetization, after detection at sensing input ZCD of falling-edge voltage at the transistor drain.

IV. EXPERIMENTAL RESULTS

Laboratory developed MTFC prototype was based on variable number (n = 2,3,6) of switch mode power supply transformers from the Würth Electronic Midcom, possessing center tapped secondary windings. The Infineon n-channel MOSFET was applied for the flyback main switch operation. Secondary Schottky rectifier diodes were connected in a way to provide symmetrical output voltages $u_{on1,2}=\pm16$ V. Photo of the MTFC prototype is in Fig. 8. Detailed parameter specification is given in Tab.II. Records of steady-state waveforms were carried out with the aid of two Tektronix oscilloscopes: the MDO4104B-3 for voltage and the DPO4034 for current channels.

Operation waveforms of the six-transformer flyback converter (6TFC) are recorded in Fig. 8 for balanced and unbalanced load conditions. In both cases, the MOSFET quasi resonant turn-on process starts at a valley of the drain voltage u_{DS}. Then, during switch turn-on interval equal distribution of primary currents i_{p1}, i_{p2} build-up is obtained. When the sum of primary currents reaches its reference value ni_{pmax}, the MOSFET is turned off. Due to low leakage inductance

Fig. 10. MTFC average output voltage regulation
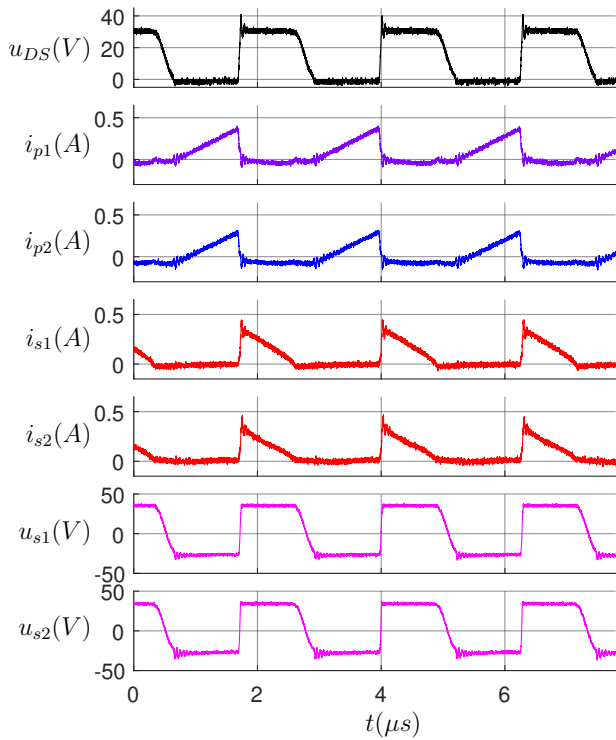
(a)
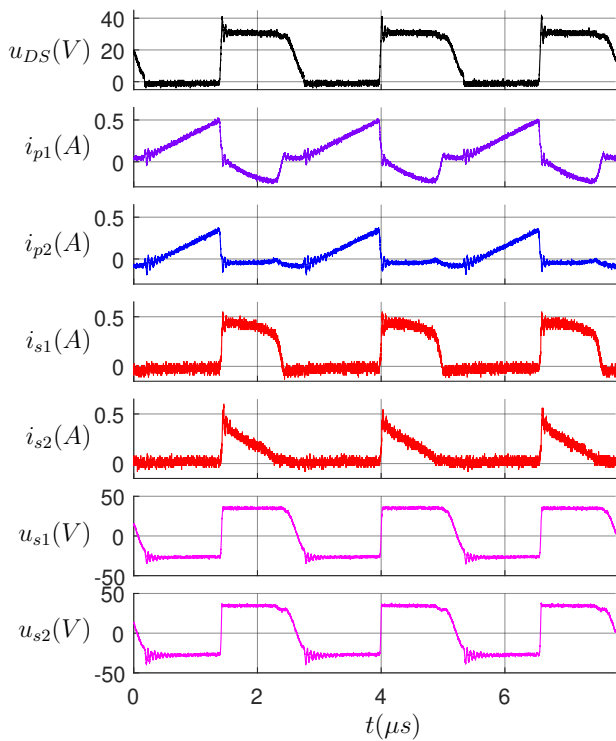
(b)

Fig. 9. The 6TFC steady-state operation; a) $R_{o1}=R_{o2}=810$ Ω, b) $R_{o1}=405$ Ω, $R_{o2}=810$ $\Omega i_p1, i_p2$

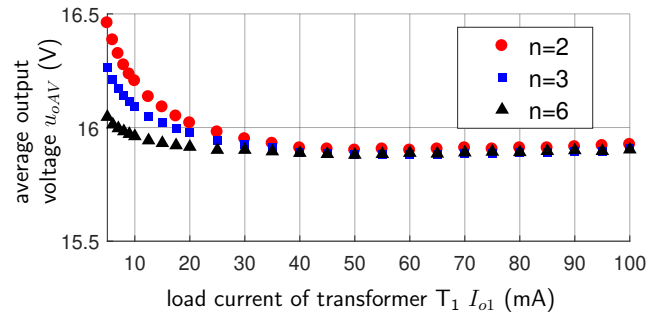L_l, that is further decreased by parallel connected primary transformer windings, and R_1DC circuit for voltage regulations, the voltage spike on the drain of the MOSFET is limited without application of auxiliary snubbers. In turn-off interval for balanced loads, secondary currents decrease to zero value simultaneously. When the load resistance R_{o1} of the first transformer T_1 is 50% reduced, a fraction of accumulated energy of each of the not overloaded units (i=2,..6) is transferred to the overload unit (i=1) by primary magnetizing currents circulating in parallel circuits. Primary and secondary current waveforms confirm analytically distinguished operation modes in the section II. The surplus power is delivered to the MTFC by augmentation of the ni_{pmax} reference in the voltage control loop. This regulation can be observed by comparing amplitudes of primary currents $i_{p1,2}$ between balanced and unbalanced conditions. From equation (20) is confirmed, that increase of ni_{pmax} reference is proportional to the increase of the total switching period T_s.

In order to validate the MTFC cross regulation quality to the transformer T_1, unit a variable resistance load was applied, while the other units were charged with the rated load resistance ($K_2=1$) corresponding to the output current $I_o=40$ mA. In Fig. 10, in accordance with the analysis for light load conditions of one output circuit, its output voltage u_{o1} increases, resulting in an increase of the average output voltage u_{oAV}. Together with increasing number of transformers the influence of output voltage u_{o1} on average value u_{oAV} is reduced. In the next Fig. 11, output voltage deviation Δu_o is measured and calculated for different number of transformers. A very good coherence between measurements and model computation (eq. 37, 38) of cross regulated voltage deviation Δu_o in function of load unbalanced factor K_2 is obtained.

In Fig. 12 is depicted the laboratory record of the transient performance of 10-transformers MTFC supplying power switch drivers (HCPL3120) of parallel quasi-resonant dc link inverter. Before inverter turn on instant the MTFC operates at no load, that is indicated by very slight oscillatory output voltage transients following flyback controller turn off periods. After inverter turn on, the load of independent MTFC outputs is increased providing stabilized output voltage operation.

To compare features of the MOFC with the MTFC, new prototypes were built and are depicted in Fig.13. The PCB surfaces' occupation is comparable for both solutions, however the height of the MOFC transformer is 2 times bigger than
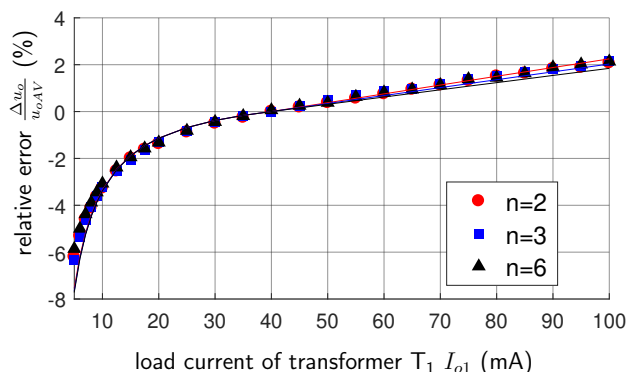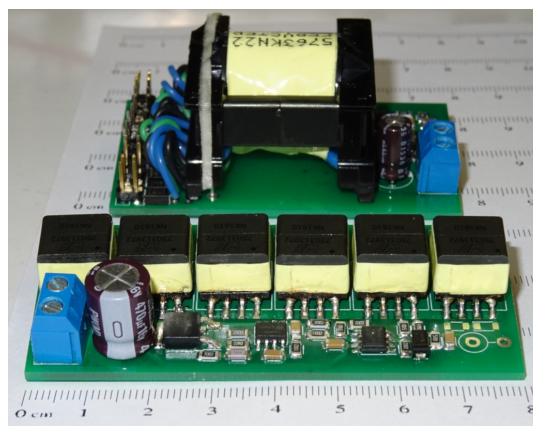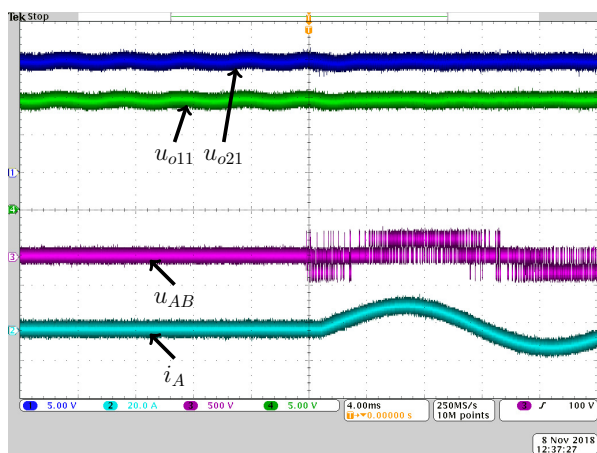
Fig. 11. MTFC relative voltage deviation

Fig. 12. 10-Transformers MTFC transient performance at the inverter turn on; u_{o11}, u_{o21} – positive output voltages in two independent channels (5V/div), u_{AB} – inverter line-to-line output voltage (500V/div), i_A – inverter output line current (20A/div)

Fig. 13. MOFC vis-à-vis MTFC for the 6 isolated symmetric supply tracks ±15 V; (prototype setup height [mm]: MOFC-26; MTFC-12,5)
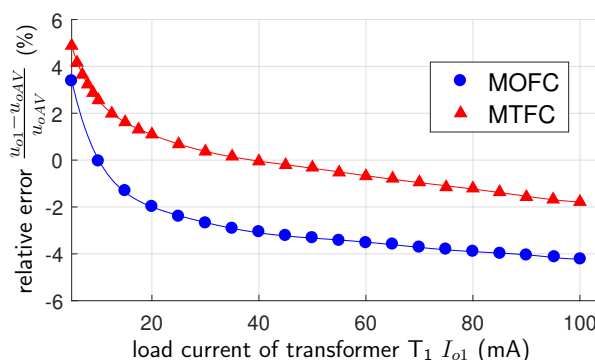

Fig. 14. Relative output voltage deviation in MTFC and MOFC

the MTFC transformer height. In Fig. 14 is measured voltage deviation at unbalanced load of the output circuit of the MOFC and the MTFC prototypes. A reduced voltage deviation for the MTFC is confirmed.

V. CONCLUSION

Described in this paper MTFC topology is characterized by parallel connection of primary windings of separate transformers instead of using multiple isolated secondary windings on the single transformer core. Such topological rearrangement of multi-output power supply provides:

- better magnetic coupling between primary and secondary circuits of each power supply track,
- better isolation between separate units,
- minimization of capacitive coupling between secondary and primary multi-transformer circuits – reducing electromagnetic interference emission of IGBT and MOSFET switching operation,
- high switching frequency operation with prospective to miniaturize the transformers volume
- reduced voltage deviation of multiple outputs by applying the primary-side average voltage regulation.

The proposed MTFC may be an alternative solution for supplying isolated IGBT and MOSFET drivers in power electronic converters with a large number of power electronic switches. This topology can be used for any combination of positive and negative voltages, depending on transformer secondary winding configuration and turns ratio.

REFERENCES

[1] R. Perret, Ed., *Power Electronics Semiconductor Devices*. Wiley-ISTE, 2009.
[2] R. M. Zwicker, "Generation of multiple isolated bias rails for IGBT inverters using flyback/sepic/cuk combination," in *PCIM Europe 2014; International Exhibition and Conference for Power Electronics, Intelligent Motion, Renewable Energy and Energy Management; Proceedings of*, pp. 1–8, May. 2014.
[3] C. Klumpner and N. Shattock, "A cost-effective solution to power the gate drivers of multilevel inverters using the bootstrap power supply technique," in *Applied Power Electronics Conference and Exposition, 2009. APEC 2009. Twenty-Fourth Annual IEEE*, DOI 10.1109/APEC.2009.4802910, pp. 1773–1779, Feb. 2009.
[4] J. Pickard, "Under the hood of flyback SMPS designs," in *2010 Texas Instruments Power Supply Design Seminar*, 2010.
[5] J. Ferrieux and F. Forest, *Alimentations à découpage, convertisseurs à résonance: principes, composants, modélisation*. Masson, 1994.
[6] C. Ji, M. Smith, K. M. Smedley, and K. King, "Cross regulation in flyback converters: analytic model and solution," *IEEE Trans. Power Electron.*, vol. 16, DOI 10.1109/63.911147, no. 2, pp. 231–239, Mar. 2001.
[7] C. Adragna, "L6565 quasi-resonant controller," AN1326 Appl. Note, 2002.

[8] T. J. . Liang, K. H. Chen, and J. F. Chen, "Primary side control for flyback converter operating in DCM and CCM," *IEEE Trans. Power Electron.*, vol. 33, DOI 10.1109/TPEL.2017.2709811, no. 4, pp. 3604–3612, Apr. 2018.

[9] P. C. Hsieh, C. J. Chang, and C. L. Chen, "A primary-side-control quasi-resonant flyback converter with tight output voltage regulation and self-calibrated valley switching," in *2013 IEEE Energy Conversion Congress and Exposition*, DOI 10.1109/ECCE.2013.6647148, pp. 3406–3412, Sep. 2013.

[10] R. Nalepa, N. Barry, and P. Meaney, "Primary side control circuit of a flyback converter," in *APEC 2001. Sixteenth Annual IEEE Applied Power Electronics Conference and Exposition (Cat. No.01CH37181)*, vol. 1, DOI 10.1109/APEC.2001.911699, pp. 542–547 vol.1, 2001.

[11] M. T. Zhang, M. M. Jovanovic, and F. C. Lee, "Design considerations and performance evaluations of synchronous rectification in flyback converters," in *Proceedings of APEC 97 - Applied Power Electronics Conference*, vol. 2, DOI 10.1109/APEC.1997.575641, pp. 623–630 vol.2, Feb. 1997.

[12] J. Zhang, H. Zeng, and X. Wu, "An adaptive blanking time control scheme for an audible noise-free quasi-resonant flyback converter," *IEEE Trans. Power Electron.*, vol. 26, DOI 10.1109/TPEL.2011.2114675, no. 10, pp. 2735–2742, Oct. 2011.

[13] J. Park, Y. J. Moon, M. G. Jeong, J. G. Kang, S. H. Kim, J. C. Gong, and C. Yoo, "Quasi-resonant (QR) controller with adaptive switching frequency reduction scheme for flyback converter," *IEEE Trans. Ind. Electron.*, vol. PP, DOI 10.1109/TIE.2016.2523931, no. 99, pp. 1–1, 2016.

[14] H. S. Kim, J. H. Jung, J. W. Baek, and H. J. Kim, "Analysis and design of a multioutput converter using asymmetrical pwm half-bridge flyback converter employing a parallel-series transformer," *IEEE Trans. Ind. Electron.*, vol. 60, DOI 10.1109/TIE.2012.2200220, no. 8, pp. 3115–3125, Aug. 2013.

[15] R. Pittini, L. Huang, Z. Zhang, and M. Andersen, "Primary parallel secondary series flyback converter (PPSSFC) with multiple transformers for very high step-up ratio in capacitive load charging applications," in *Applied Power Electronics Conference and Exposition (APEC), 2014 Twenty-Ninth Annual IEEE*, DOI 10.1109/APEC.2014.6803496, pp. 1440–1447, Mar. 2014.

[16] D. von den Hoff, K. Oberdieck, and R. W. D. Doncker, "A multi-output resonant gate-driver power supply for electric vehicle applications," in *2017 IEEE 12th International Conference on Power Electronics and Drive Systems (PEDS)*, DOI 10.1109/PEDS.2017.8289215, pp. 1,214–1,218, Dec. 2017.

[17] M. Kolincio, P. J. Chrzan, and P. Musznicki, "Multi-transformer flyback converter for supplying isolated IGBT and MOSFET drivers," in *2016 10th International Conference on Compatibility, Power Electronics and Power Engineering (CPE-POWERENG)*, DOI 10.1109/CPE.2016.7544226, pp. 428–432, Jun. 2016.

[18] Linear Technology Corporation, "LTspice XVII," http://www.linear.com/designtools/software/, 2017.

Maciej Kolincio (S'18) was born in Gdansk, Poland in 1990. He received the B.Sc.(Eng.) degree and M.Sc. degree in electrical engineering from Gdansk University of Technology, Gdansk, Poland in 2013 and 2014 respectively, where he is currently finishing his Ph.D studies. His research interest focuses on power electronics, including multi-output dc/dc converters.

Piotr J. Chrzan (SM'14) received the M.S. degree in electronic engineering and the Ph.D., Dr.Sc. degrees in electrical engineering from Gdansk University of Technology, Gdansk, Poland, in 1978, 1988, and 1999 respectively.

Since 1980, he has been with the Faculty of Electrical and Control Engineering, Gdansk University of Technology, where he was the Vice-Dean of the Faculty (2008-2012), and General Co-Chair of the International Symposium on Industrial Electronics (IEEE-ISIE 2011). He has held several Visiting Professor positions at the National Polytechnic Institute of Toulouse and the University of Poitiers, France. He has been an Invited Researcher several times at the Grenoble Electrical Engineering Laboratory, France.

Since 2017, he has been a Professor and Chair of Power Electronics and Electrical Machines. His research interests include high-frequency converters, modeling, control of renewable energy systems and electromagnetic compatibility. Prof. Chrzan is an Associate Editor of the IEEE TRANSACTIONS ON INDUSTRIAL INFORMATICS.

Piotr Musznicki was born in Slupsk, Poland, in 1976. He received the M.Sc. and Ph.D. degrees in power electronics from the Faculty of Electrical and Control Engineering, Gdansk University of Technology, Gdansk, Poland, in 2001 and 2006, and the Ph.D. degree from the Laboratoire d'Electrotechnique de Grenoble, Grenoble Institute of Technology (INPG), Grenoble, France, in 2006.

He is currently with Gdansk University of Technology, where he is engaged in power electronics. His current research interests include electromagnetic compatibility, modeling and controlling of the power electronics converters and electrical machines, and DSP.